

April 1999

# Magnetic and structural properties of Mg–Co nanostructures fabricated

E.M. Kirkpatrick

*University of Nebraska - Lincoln*

Diandra Leslie-Pelecky

*University of Nebraska -- Lincoln, diandra2@unl.edu*

S.-H. Kim

*University of Nebraska - Lincoln*

R.D. Rieke

*University of Nebraska - Lincoln*

Follow this and additional works at: <http://digitalcommons.unl.edu/physicslesliepelecky>



Part of the [Physics Commons](#)

---

Kirkpatrick, E.M.; Leslie-Pelecky, Diandra; Kim, S.-H.; and Rieke, R.D., "Magnetic and structural properties of Mg–Co nanostructures fabricated" (1999). *Diandra Leslie-Pelecky Publications*. 11.

<http://digitalcommons.unl.edu/physicslesliepelecky/11>

This Article is brought to you for free and open access by the Research Papers in Physics and Astronomy at DigitalCommons@University of Nebraska - Lincoln. It has been accepted for inclusion in Diandra Leslie-Pelecky Publications by an authorized administrator of DigitalCommons@University of Nebraska - Lincoln.

# Magnetic and structural properties of Mg–Co nanostructures fabricated by chemical synthesis

E. M. Kirkpatrick<sup>a)</sup> and Diandra L. Leslie-Pelecky

*Department of Physics & Astronomy and Center for Materials Research & Analysis,  
University of Nebraska, Lincoln, Nebraska 68588-0111*

S.-H. Kim and R. D. Rieke

*Department of Chemistry and Center for Materials Research & Analysis, University of Nebraska, Lincoln,  
Nebraska 68588-0304*

Reductive chemical synthesis is a versatile tool for fabricating elemental nanostructures; however, less work has been completed on understanding and controlling alloy formation. Magnetic Mg–Co and Mg–Co–C nanocomposites have been fabricated using a reductive chemical synthesis designed to produce highly active metals. The as-synthesized powder was annealed at temperatures from 150 to 650 °C. Samples were investigated using x-ray diffraction, alternating gradient force magnetometry, and superconducting quantum interference device magnetometry. X-ray diffraction indicates that the resulting structures are multiphase with MgCo<sub>2</sub>, MgCo<sub>3</sub>C<sub>0.5</sub>, fcc Co, Mg, MgO, and Li<sub>2</sub>CO<sub>3</sub> present depending on annealing temperature. The temperature-dependent magnetization of the as-synthesized sample indicates ferromagnetic and antiferromagnetic or ferrimagnetic contributions. Increases in coercivity and remanance ratio with increasing annealing temperature are consistent with the formation and growth of small Co grains. © 1999 American Institute of Physics. [S0021-8979(99)22308-0]

## I. INTRODUCTION

The Rieke chemical synthesis technique produces highly reactive metal powders by reducing metal salts in ethereal or hydrocarbon solvents using alkali metals. This technique has been employed successfully to prepare elemental nanostructured materials including zinc, aluminum, manganese, magnesium, nickel, cobalt, and others.<sup>1–3</sup> The Mg–Co system was chosen for testing the application of the Rieke technique to the production of alloys, as the x-ray diffraction peaks of the individual elements are easily distinguishable from the x-ray diffraction peaks of the alloy. Previous studies<sup>4–6</sup> have shown that both amorphous Mg<sub>x</sub>Co<sub>1–x</sub> (with  $x < 0.82$ ) and crystalline MgCo<sub>2</sub> are ferromagnetic at room temperature. This study investigates the magnetic properties of chemically synthesized Mg<sub>x</sub>Co<sub>1–x</sub> nanostructures and evaluates the potential of the Rieke technique for fabricating alloys.

## II. SYNTHESIS

Anhydrous magnesium chloride and cobalt iodide were reduced by lithium using naphthalene as an electron carrier according to:



All manipulations of the raw materials and synthesized powders were carried out under an argon atmosphere. The black slurry resulting from this reaction was centrifuged to separate the powder from the supernatant. The powder was then washed three times using freshly distilled tetrahydrofuran (THF) to remove LiI and LiCl. The slurry was dried under vacuum at room temperature, leaving a black powder. The

yield ratio—the measured mass divided by the mass obtained if all salts are reduced—is 0.39, suggesting that some of the product was left in solution after centrifuging or that some of the MgCl<sub>2</sub> or CoI<sub>2</sub> did not react and was removed by the postsynthesis washing.

## III. EXPERIMENTAL DETAILS

X-ray diffraction (XRD) was performed using a Rigaku *D-Max B* diffractometer. Mg–Co powder was mounted by forming a slurry of powder in THF on a low-background quartz sample holder, then allowing the THF to evaporate. Magnetization measurements were made using an alternating gradient force magnetometer at room temperature and a superconducting quantum interference device (SQUID) magnetometer at low temperature. Samples for magnetic measurement were placed in paraffin-filled polyethylene bags (to prevent oxidation) and sealed in an argon atmosphere. The paraffin was then melted to immobilize the particles and prevent whole-particle motion.

## IV. RESULTS AND DISCUSSION

### A. Structural properties

The highly pyrophoric nature of the as-synthesized powder precludes measurement of a x-ray diffraction pattern; however, low annealing temperatures ( $\leq 150$  °C) reduce reactivity without causing significant grain growth.<sup>3</sup> Mg–Co powders are stable in air after annealing in a vacuum of  $10^{-6}$  Torr for 1 h at temperatures between 150 and 650 °C. X-ray diffraction patterns sometimes show evidence of oxidation; however, the powders are exposed to air during the XRD measurement and oxidation can occur during the measurement.

<sup>a)</sup>Electronic mail: emk@unlinfo.unl.edu

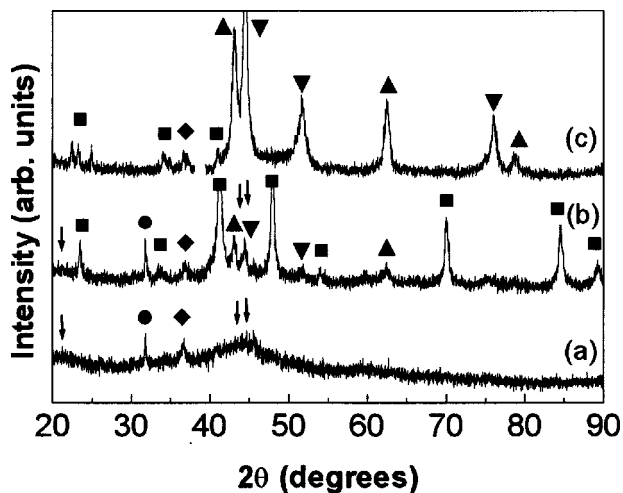


FIG. 1. XRD patterns of Mg–Co nanocomposites annealed for 1 h at (a) 150, (b) 250, and (c) 650 °C. Arrows denote  $\text{MgCo}_2$  peak positions. Diffraction peaks corresponding to  $\text{MgCo}_3\text{C}_{0.5}$  are denoted by squares,  $\text{Li}_2\text{CO}_3$  by circles, Mg by diamonds, MgO by triangles, and fcc Co by inverted triangles.

Figure 1 shows the XRD patterns of samples annealed at 150 (a), 250 (b), and 650 °C (c) for 1 h. Arrows identify the expected positions of the three most intense XRD peaks of  $\text{MgCo}_2$ , which is the only alloy in the Mg–Co phase diagram. The broad peaks observed in pattern (a) are characteristic of the small grain sizes (<5 nm) produced by the Rieke synthesis. The peak at 36.7° is due to Mg, and is consistent with a mixture of  $\text{MgCo}_2$  and excess Mg resulting from the initial 1:1 ratio of Mg salt to Co salt. The peak at 31.8° is due to  $\text{Li}_2\text{CO}_3$ , which is observed in other samples made using the Rieke technique.<sup>2</sup> The metals produced by the Rieke synthesis are reactive enough to cleave the solvent molecules, thus incorporating carbon in the final product.

Annealing at temperatures above 150 °C, but below 650 °C, produces a multiphase nanocomposite that is typified by pattern (b) in Fig. 1. A diffraction peak that corresponds to the 100% intensity  $\text{MgCo}_2$  peak is observed; however, the position at which the 85% intensity  $\text{MgCo}_2$  peak would be observed is obscured by diffraction peaks attributable to other phases. The peak at 21.1° (70% intensity) is not observed at all, so  $\text{MgCo}_2$  may not be present in this sample.

The XRD peaks identified by squares correspond to  $\text{MgCo}_3\text{C}_{0.5}$ . Carbonization occurs due to the incorporation of solvent fragments during synthesis. The Mg–Co phase diagram contains no fcc phases; however, carbon stabilizes<sup>7</sup> the fcc compound  $\text{MgCo}_3\text{C}_{0.5}$ . The XRD peaks corresponding to  $\text{MgCo}_3\text{C}_{0.5}$  are shifted to the right by 0.3° at low angles. The shift becomes larger at higher angles, with a maximum shift of 0.7°. The other peaks in pattern (b) correspond to  $\text{Li}_2\text{CO}_3$ , fcc Co, Mg, and MgO. Shifts (~0.3°) are observed in the fcc Co peaks, but not in the Mg, MgO, or  $\text{Li}_2\text{CO}_3$  peaks. The unshifted peaks suggest that the observed shifts are not the result of systematic measurement error. Strain may be responsible for the shifts, which are also present in annealed samples. There is no change in the phases present in samples annealed between 250 and 550 °C, however, there is a noticeable increase in the amount of fcc cobalt relative to the

TABLE I. Phases present for samples annealed at various temperatures. (✓= present, ?= may be present, X=not present).

	150 °C	250 °C	450 °C	550 °C	650 °C
$\text{MgCo}_2$	✓	?	?	?	?
$\text{Li}_2\text{CO}_3$	✓	✓	✓	X	X
Mg	✓	✓	✓	✓	✓
MgO	X	✓	✓	✓	✓
$\text{MgCo}_3\text{C}_{0.5}$	X	✓	✓	✓	✓
fcc Co	X	✓	✓	✓	✓

other components with increasing annealing temperature.

Pattern (c) of Fig. 1 shows that annealing at 650 °C diminishes the intensities of the  $\text{MgCo}_3\text{C}_{0.5}$  peaks relative to MgO and fcc Co.  $\text{Li}_2\text{CO}_3$  is no longer observed in the XRD pattern. All fcc Co peaks between 20° and 90° are observed in pattern (c) and exhibit a small (0.1°–0.2°) shift to higher angles. Mg and MgO remain after annealing. The peaks at 22.5° and 24.9° are currently unidentified. Table I summarizes the phases present at each annealing temperature.

## B. Magnetic properties

Placing the samples in paraffin-filled bags sealed under argon allows measurement of all Mg–Co samples, including the pyrophoric as-synthesized powder. Figure 2 shows the room-temperature hysteresis loop for the as-synthesized Mg–Co powder. The saturation magnetization,  $M_s$ , of the as-synthesized sample is 62 emu/g with a saturating field of 10–15 kOe. The coercivity is 35 Oe and the remanance ratio is 0.04.  $M_s$  of the as-synthesized sample is higher than the value obtained for crystalline<sup>5</sup>  $\text{MgCo}_2$  (57 emu/g) and lower than the value obtained for amorphous  $\text{Mg}_{1-x}\text{Co}_x$  for  $x = 0.5$  (76 emu/g).<sup>6</sup> The presence of additional, nonmagnetic phases and/or superparamagnetic contributions complicates comparison to bulk systems.

Figure 3 shows the magnetization at 55 kOe as a function of temperature for as-synthesized Mg–Co. The data are fit to a combination of a Bloch law and a Curie–Weiss law:

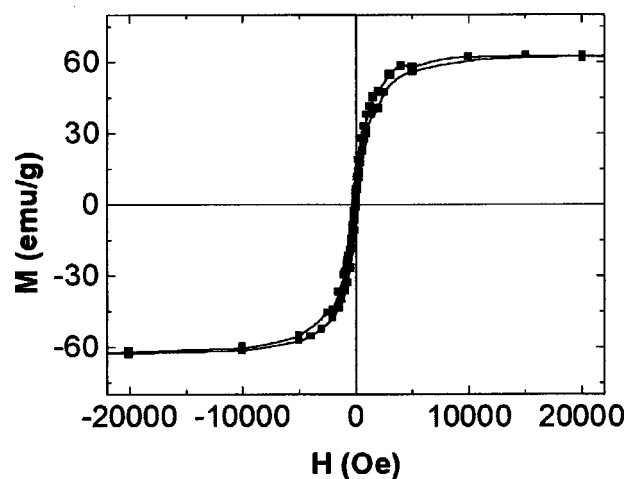


FIG. 2. Magnetization of as-synthesized Mg–Co as a function of applied field at room temperature.

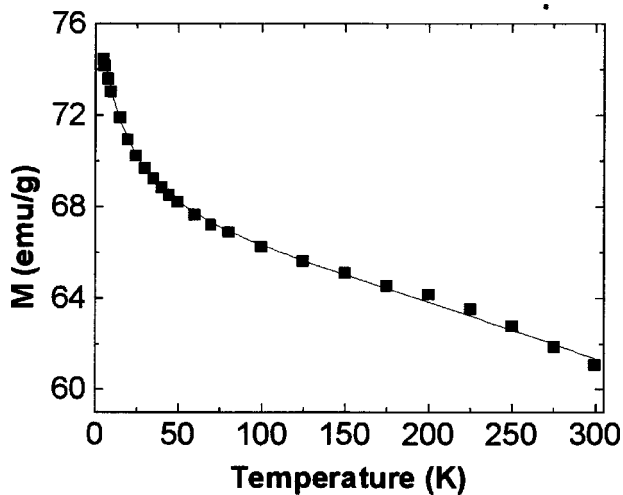


FIG. 3. Magnetization of as-synthesized Mg-Co as a function of temperature in an applied field of 55 kOe.

$$M = M_o(1 + BT^{3/2}) + \frac{CH}{(T - \Theta)}, \quad (2)$$

where  $M_o = M(T=0)$ ,  $B$  is the Bloch constant,  $C$  is the Curie constant,  $H$  is the applied field, and  $\Theta$  measures the magnetic interaction strength. The solid line in Fig. 3 represents a fit to Eq. (2), with  $M_o = 65(\pm 2)$  emu/g,  $B = -1.4(\pm 0.1) \times 10^{-5} \text{ K}^{-3/2}$ ,  $C = 3.8(\pm 0.3) \times 10^{-3} \text{ emu K}/(\text{g Oe})$ , and  $\Theta = -18(\pm 2) \text{ K}$ . A negative value for  $\Theta$  can indicate the presence of antiferromagnetic or ferrimagnetic components.<sup>8</sup> MgCo<sub>2</sub> becomes antiferromagnetic at 45 K and could account for the sign of  $\Theta$ .<sup>5</sup> Small amounts of CoO undetectable by XRD would also affect magnetic behavior; however, no shifts are seen in field-cooled hysteresis loops.

Figure 4 shows the coercivity ( $H_c$ ) and remanance ratio ( $M_r/M_s$ ) as functions of annealing temperature.  $H_c$  and  $M_r/M_s$  remain relatively constant for annealing tempera-

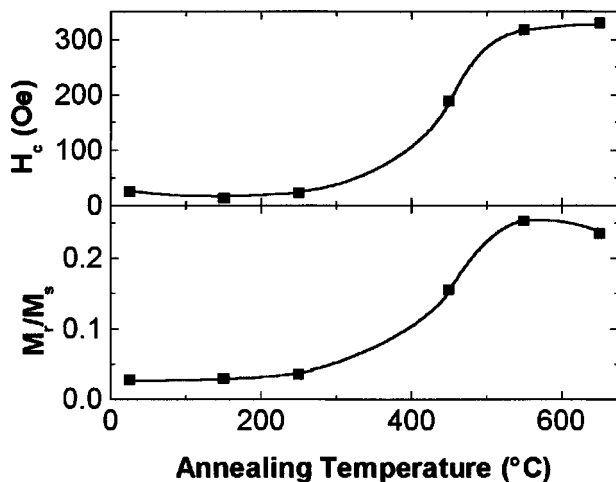


FIG. 4. Coercivity and remanance ratio of Mg-Co nanostructures as functions of annealing temperature.

tures  $\leq 250^\circ\text{C}$ . Samples annealed at  $T \geq 450^\circ\text{C}$  have larger coercivities and remanance ratios, with maximum values  $H_c = 328 \text{ Oe}$ , and  $M_r/M_s = 0.25$ . The presence of multiple phases that depend strongly on temperature complicates interpretation of magnetic data; however, the significant changes in  $H_c$  and  $M_r/M_s$  occur between 250 and  $550^\circ\text{C}$ . XRD over this temperature range shows that the same phases are present, but that the amount of fcc Co increases noticeably with increasing annealing temperature. An increase in  $M_s$  is also observed in samples showing evidence of Co particles. Increases in  $H_c$  and  $M_r/M_s$  with annealing temperature are consistent with the formation and growth of fcc cobalt. Fine Co grains<sup>3</sup> can produce higher coercivities than both amorphous Mg-Co<sup>4</sup> and crystalline MgCo<sub>2</sub>.<sup>5</sup> The Scherrer equation applied to the cobalt XRD peaks yields a diffracting crystallite size of  $\sim 7 \text{ nm}$  for the sample annealed at  $550^\circ\text{C}$  and  $\sim 10 \text{ nm}$  for the sample annealed at  $650^\circ\text{C}$ . The values obtained for the coercivity are consistent with the values measured in fine-particle cobalt systems with comparable grain sizes.<sup>9,10</sup>

## V. CONCLUSION

The formation of alloys using the Rieke synthesis technique has been demonstrated; however, the extreme reactivity of the metals produced results in a complex, multiphase nanostructure.  $M_s$  of the as-synthesized powder is between the reported values for crystalline MgCo<sub>2</sub> and amorphous MgCo; however, the presence of nonmagnetic components has not been quantitatively considered. The temperature-dependent magnetization of the as-synthesized sample shows the presence of a ferromagnetic component and an antiferromagnetic or ferrimagnetic component.  $H_c$  and  $M_r/M_s$  increase with increasing annealing temperature and are consistent with the formation and growth of fcc cobalt grains (with sizes on the order of 10 nm). Further study of the sample morphology and investigation of the temperature dependence of the magnetization are necessary to improve our understanding of the correlation between nanostructure and magnetism in these chemically synthesized materials.

<sup>1</sup>Reuben D. Rieke, *Crit. Rev. Surf. Chem.* **1**, 131 (1991).

<sup>2</sup>D. L. Leslie-Pelecky, S.-H. Kim, M. Bonder, X. Q. Zhang, and R. D. Rieke, *Chem. Mater.* **10**, 164 (1998).

<sup>3</sup>D. L. Leslie-Pelecky, M. Bonder, T. Martin, E. M. Kirkpatrick, X. Q. Zhang, S.-H. Kim, and R. D. Rieke, *IEEE Trans. Magn.* **34**, 1018 (1998).

<sup>4</sup>S. Prasad, R. Krishnan, and M. Tessier, *IEEE Trans. Magn.* **MAG-22**, 1113 (1986).

<sup>5</sup>K. H. J. Buschow, *Solid State Commun.* **17**, 891 (1975).

<sup>6</sup>K. H. J. Buschow and P. G. van Engen, *Solid State Commun.* **39**, 1 (1981).

<sup>7</sup>L. J. Huetter and H. H. Stadelmaier, *Acta Metall.* **6**, 367 (1958).

<sup>8</sup>B. D. Cullity, *Introduction to Magnetic Materials* (Addison-Wesley, Reading, MA, 1972).

<sup>9</sup>T. Hayashi, S. Hirono, M. Tomita, and S. Umemura, *Nature (London)* **381**, 772 (1996).

<sup>10</sup>S. Gangopadhyay, G. C. Hadjipanayis, C. M. Sorensen, and K. J. Klumbunde, *IEEE Trans. Magn.* **29**, 2602 (1993).